Lanthanum Complexes Containing a Bis(phenolate) Ligand with a Ferrocenediyl-1,1'-dithio Backbone: Synthesis, Characterization, and Ring-opening Polymerization of *rac*-Lactide

*Catherine Hermans, Weifeng Rong, Thomas P. Spaniol and Jun Okuda**

*Institute of Inorganic Chemistry, RWTH Aachen University, Landoltweg 1, D-52056 Aachen, Germany.
E-mail: jun.okuda@ac.rwth-aachen.de

Table of Contents

1. NMR Spectra of Complex [(L)LaN(SiMe$_3$)$_2$] (1)

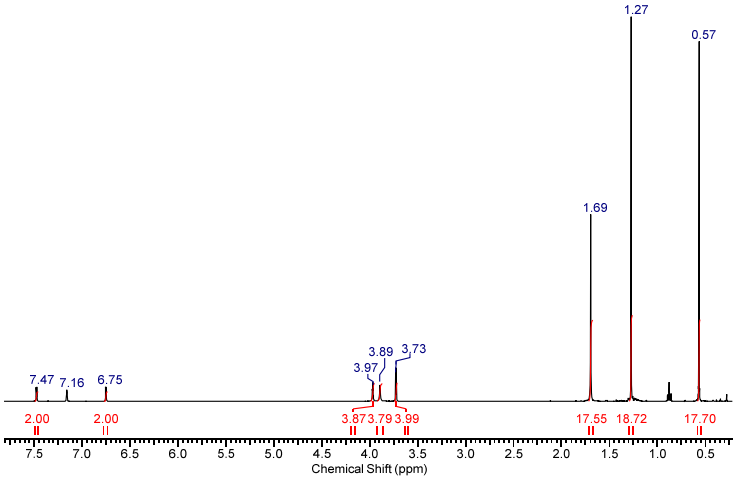

Fig. S1 ^{1}H NMR spectrum (C_6D_6, 400 MHz) of complex [(L)LaN(SiMe$_3$)$_2$] (**1**).

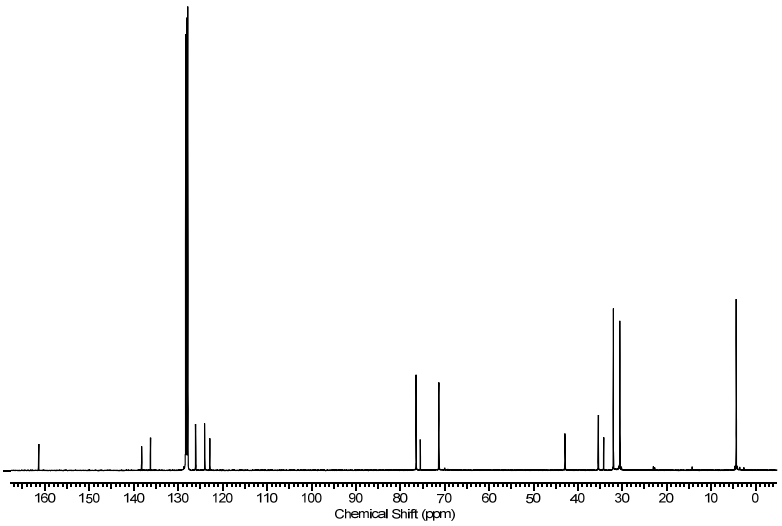

Fig. S2 ^{13}C {^{1}H} NMR spectrum (C_6D_6, 101 MHz) of complex **1**.

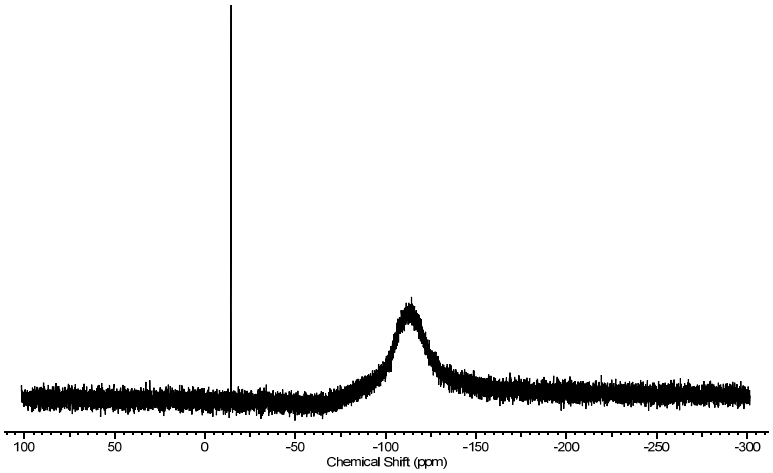

Fig. S3 ^{29}Si {^{1}H} NMR spectrum (C_6D_6, 79.5 MHz) of complex **1**.

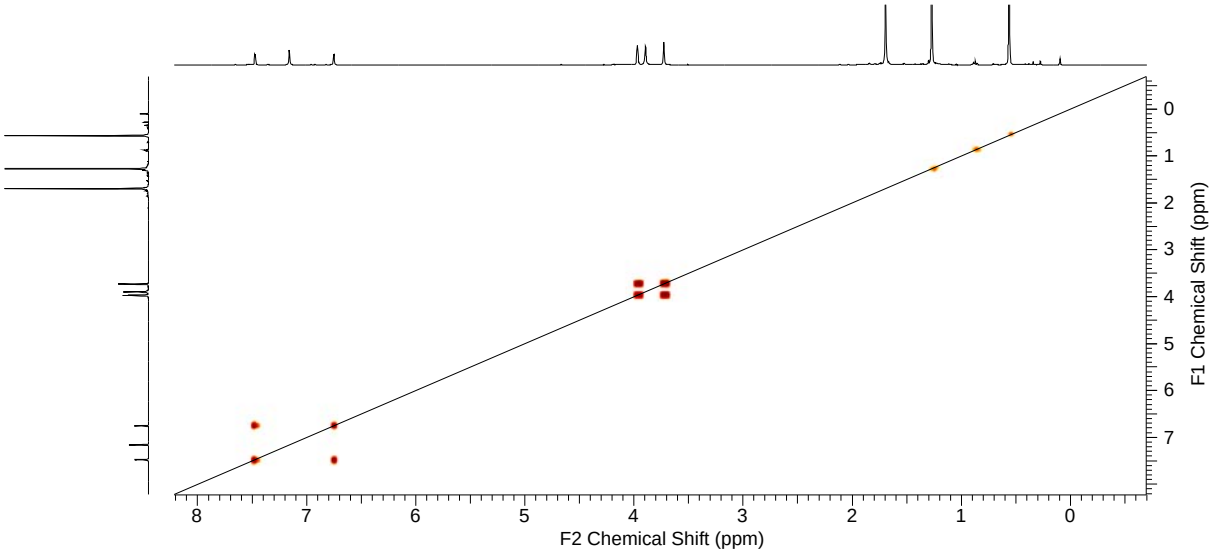

Fig. S4 Homonuclear correlation spectroscopy (COSY) of complex **1** (in C_6D_6).

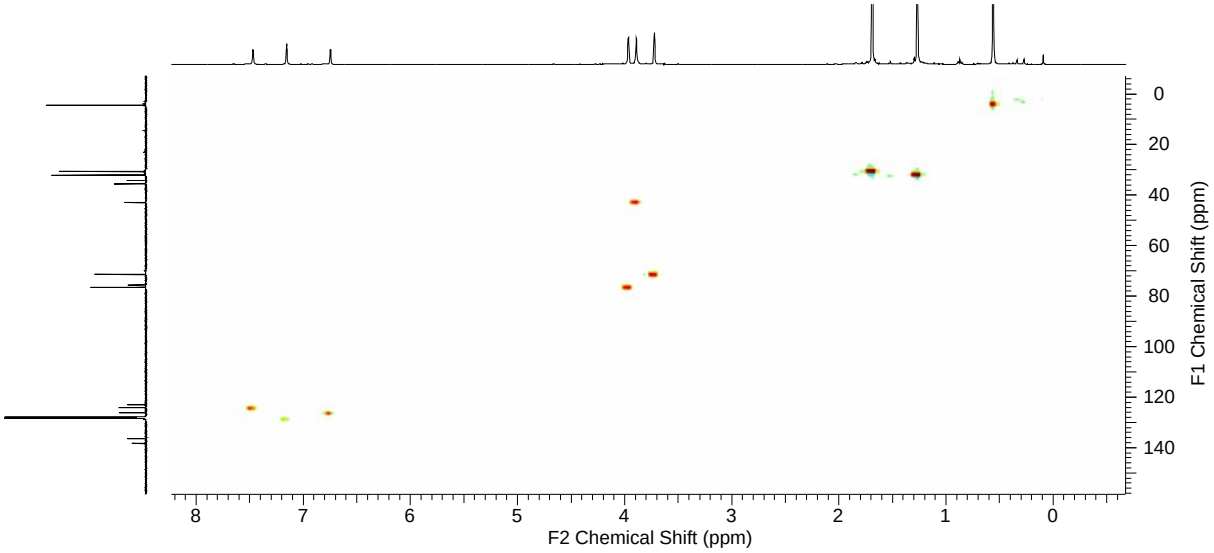

Fig. S5 ^{1}H-^{13}C Heteronuclear single quantum correlation (HSQC) experiment of complex **1** (in C_6D_6).

2. NMR Spectra of Complex [(L)LaO^{i}Pr] (2)

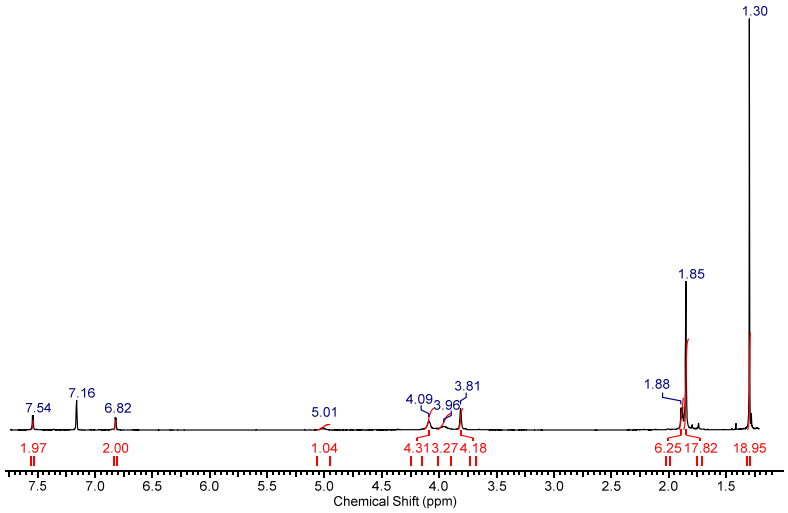

Fig. S6 ^{1}H NMR spectrum (C_6D_6, 400 MHz) of complex [(L)LaO^{i}Pr] (**2**).

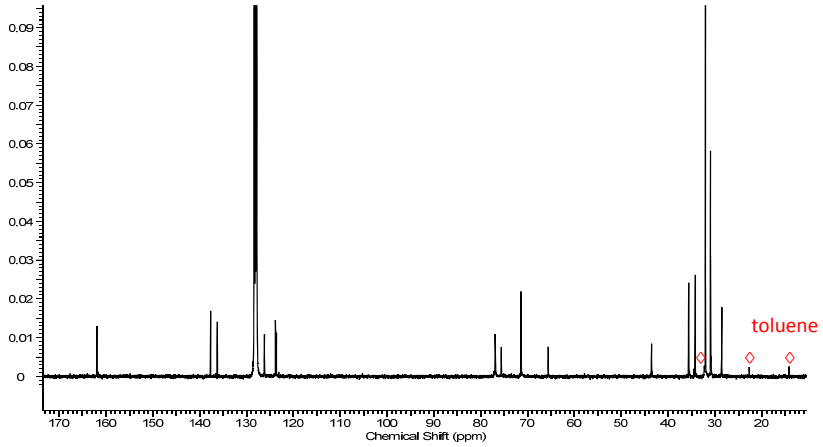

Fig. S7 ^{13}C {^{1}H} NMR spectrum (C_6D_6, 101 MHz) of complex **2**.

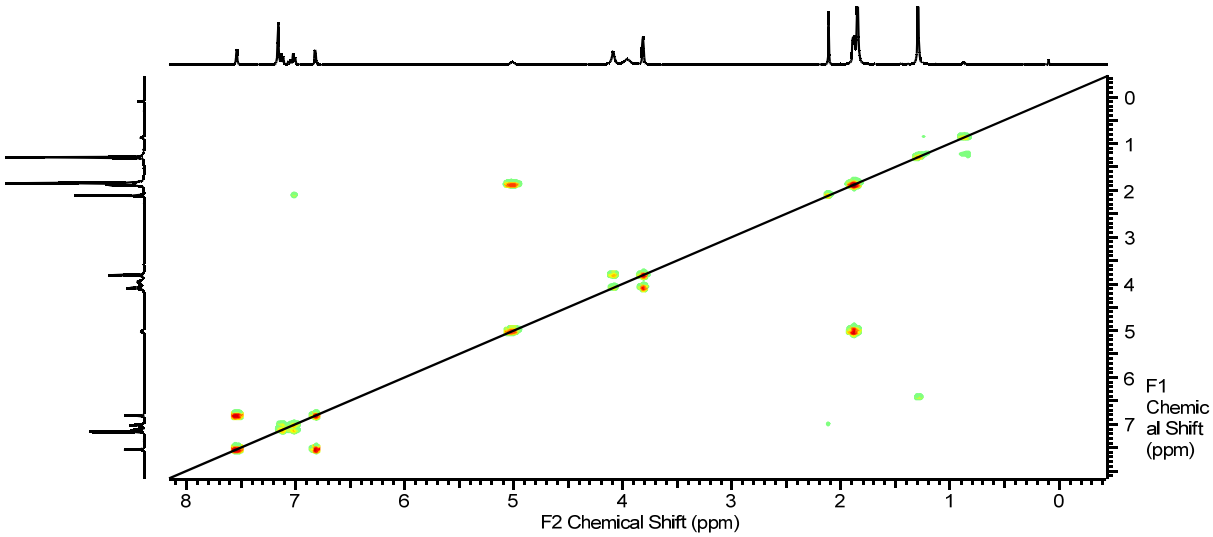

Fig.S8 Homonuclear correlation spectroscopy (COSY) of complex **2** (in C_6D_6, containing toluene residue).

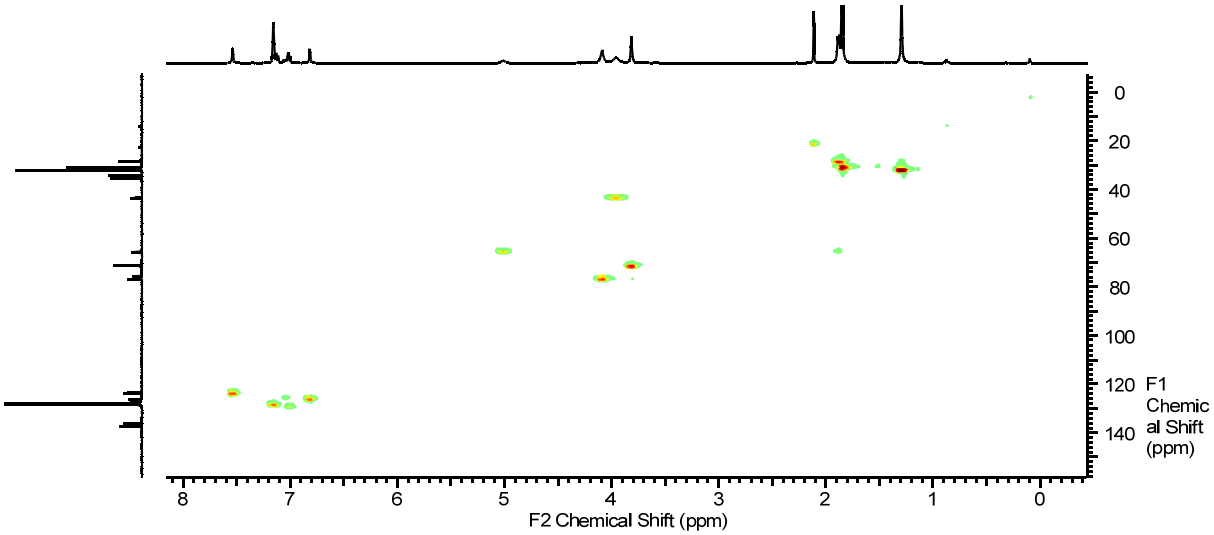

Fig. S9 ^{1}H-^{13}C Heteronuclear single quantum correlation (HSQC) experiment of complex **2** (in C_6D_6, containing toluene residue).

3. NMR Spectra of Complex [(L)LaBH$_4$] (3)

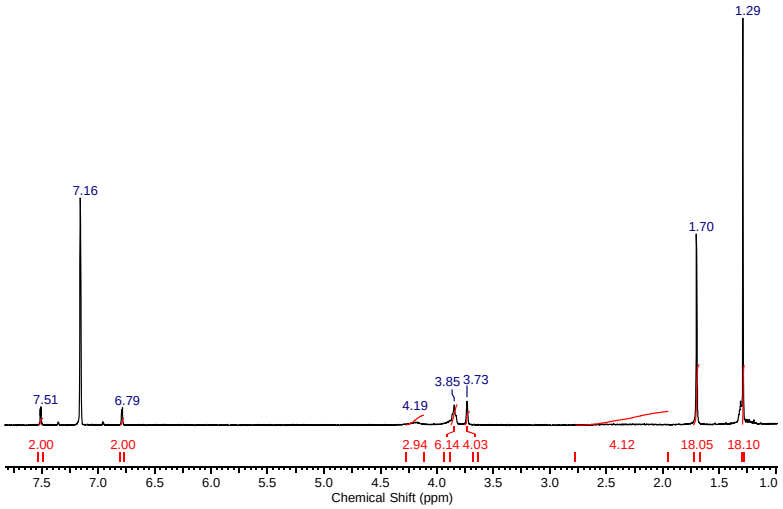

Fig. S10 ^{1}H NMR spectrum (C_6D_6, 400 MHz) of complex [(L)LaBH$_4$] (**3**).

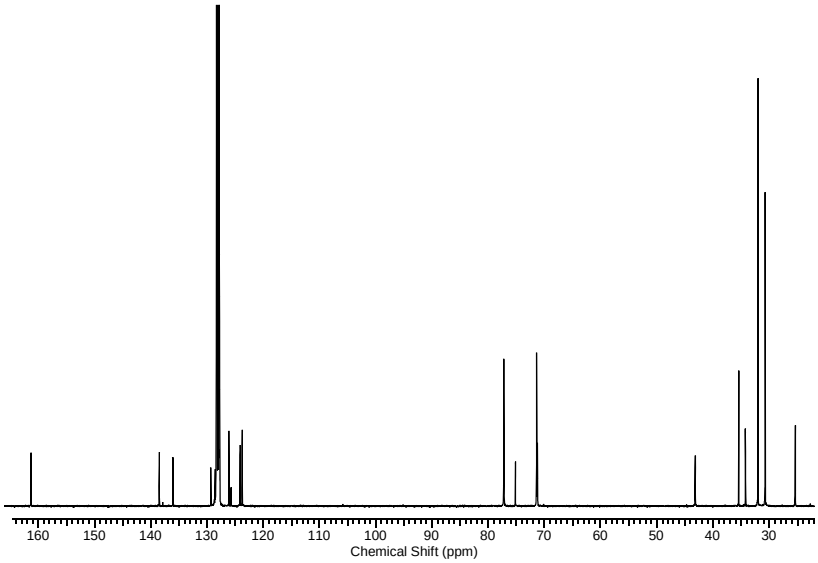

Fig. S11 ^{13}C {^{1}H} NMR spectrum (C_6D_6, 101 MHz) of complex **3**.

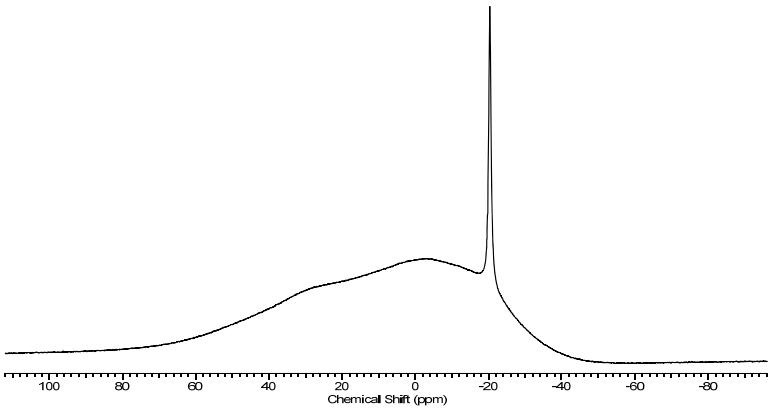

Fig. S12 ^{11}B {^{1}H} NMR spectrum (C_6D_6, 128.4 MHz) of complex **3**.

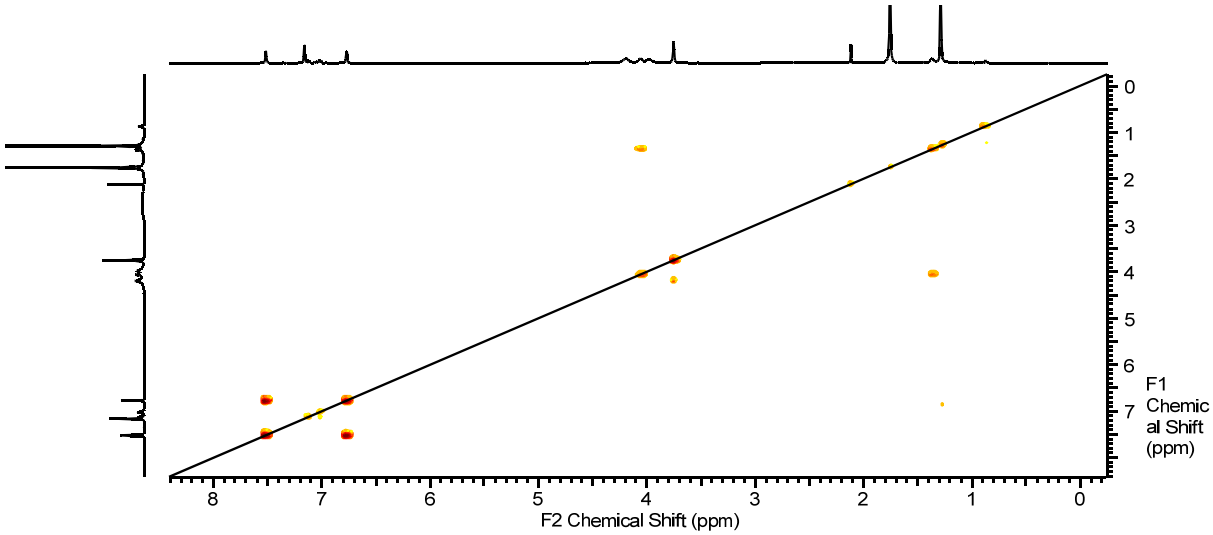

Fig. S13 Homonuclear correlation spectroscopy (COSY) of complex **3** (in C_6D_6, containing toluene residue).

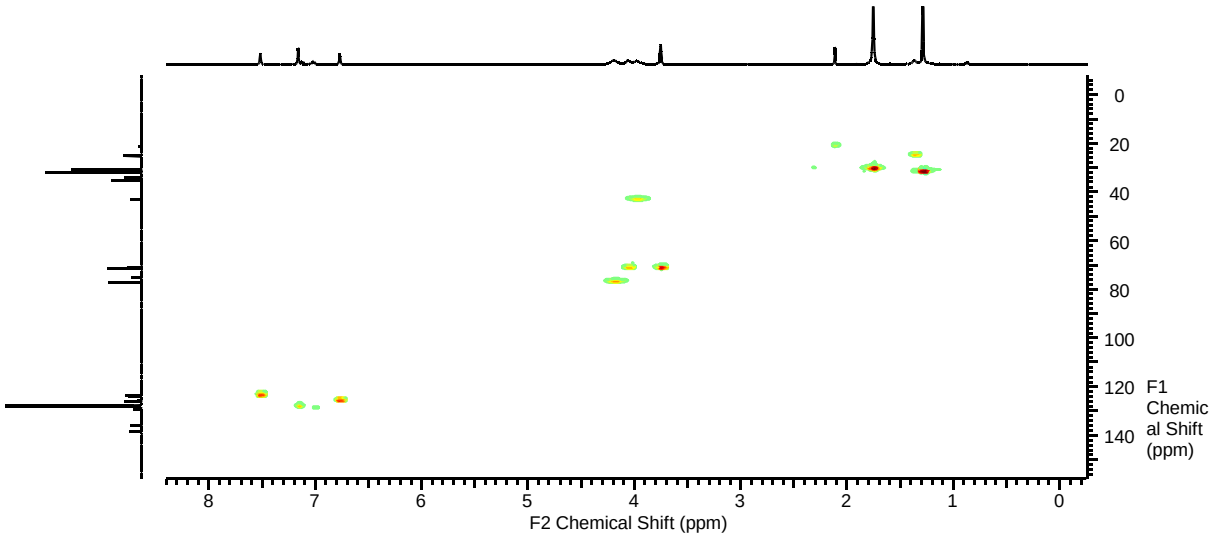

Fig. S14 ^{1}H-^{13}C Heteronuclear single quantum correlation (HSQC) experiment of complex **3** (in C_6D_6, containing toluene residue).

4. Polymerization Kinetics

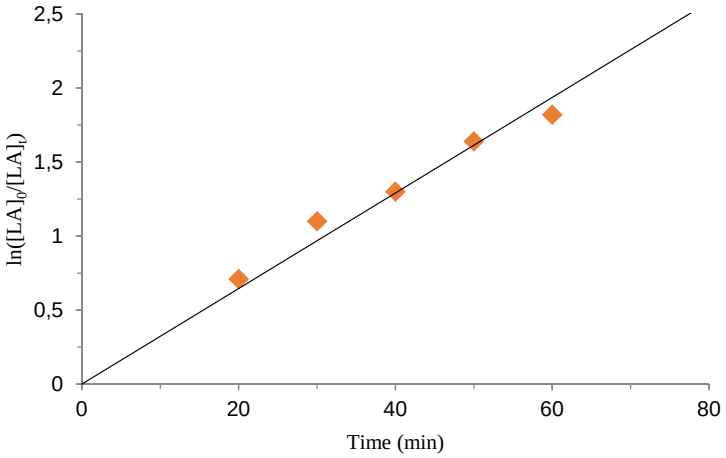

Fig. S15 First-order kinetic plot for the polymerization of *rac*-LA in THF at 25 °C with complex **1** as initiator (THF = 6 mL, $[M]_0$ = 0.5 M, [I] = 0.833 mM, k_{app} = 0.032 min^{-1}).

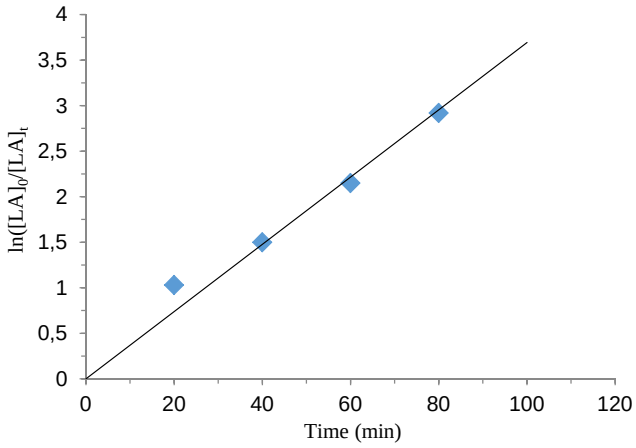

Fig. S16 First-order kinetic plot for the polymerization of *rac*-LA in THF at 25 °C with complex **2** as initiator (THF = 6 mL, $[M]_0$ = 0.5 M, [I] = 0.833 mM, k_{app} = 0.036 min^{-1}).

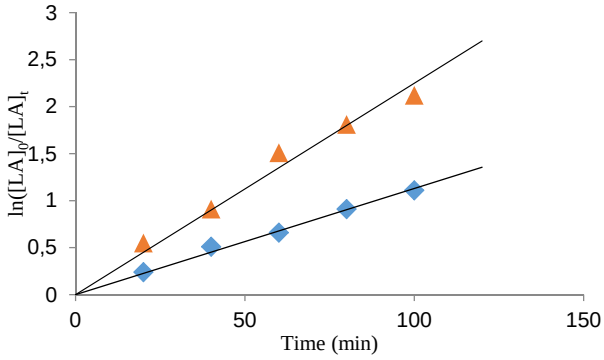

Fig. S17 First-order kinetic plots for the polymerization of *rac*-LA in THF at 60 °C with complex **3** as initiator (triangle: THF = 2 mL, $[M]_0$ = 1 M, [I] = 5 mM, k_{app} = 0.022 min^{-1}; square: THF = 4 mL, $[M]_0$ = 0.5 M, [I] = 2.5 mM, k_{app} = 0.011 min^{-1}).

5. Polymerization Kinetics

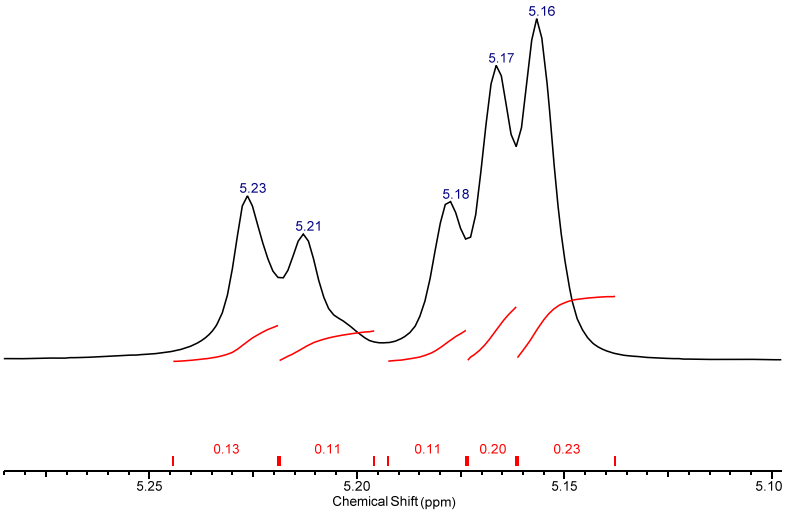

Fig. S18 ^{1}H $\{^{1}H\}$ NMR spectrum of PLA (sample Table 2, Entry 6) in $CDCl_3$.

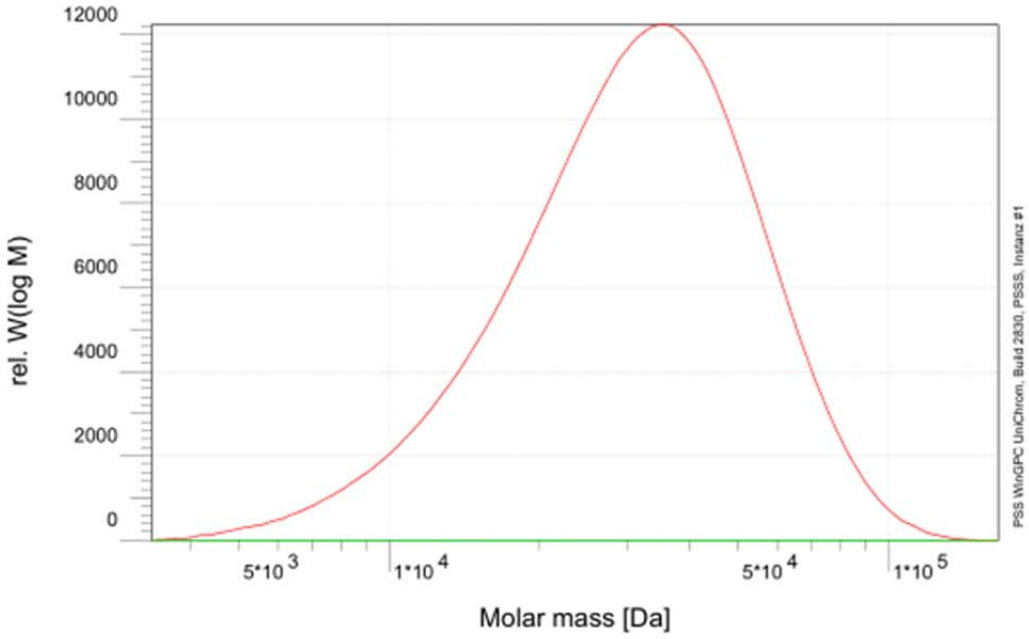

Probe :	Vial 2: WR/518/4 - 1		
Integration von :	Dienstag 19.05.15 10:16:04		21.236 ml
Integration bis :	Dienstag 19.05.15 10:23:27		28.821 ml
Kalibration :	thf20132406.CAL	**Eluent :**	THF
MHK - A (Kal.):	1.000E+0	**MHK - K (Kal.):**	0.000E+0 ml/g
Int.Stand.-K :	37.250 ml	**Int.Stand.-M :**	36.300 ml
Pumpe :	PSS SECcurity	**Flußrate :**	1.000 ml/min
Konzentration :	0.000 g/l	**Injektvolumen :**	20.000 ul
Säule 1 :	PSS SDV 5µm	**Temperatur :**	25.000 °C
Säule 2 :	PSS SDV 5µm	**Temperatur :**	25.000 °C
Säule 3 :	PSS SDV 5µm	**Temperatur :**	25.000 °C
Detektor 1 :	I1: RID 1, RI Signal	**Versatz :**	0.217 ml
Detektor 2 :	I1: VWD 1, Signal A	**Versatz :**	0.000 ml
Operateur :	mpaul	**Messintervall :**	1.000 sec

	I1: RID 1, RI Signal		**I1: VWD 1, Signal A**		
		Unsicherheit [%]		**Unsicherheit [%]**	
Mn :	2.5153e4	11.92	1.3036e4	n/v	g/mol
Mw :	3.4830e4	11.92	2.9148e4	n/v	g/mol
Mz :	4.4841e4	11.92	5.5166e4	n/v	g/mol
Mv :	3.4830e4	11.92	2.9148e4	n/v	g/mol
D :	1.3848e0	16.85	2.2359e0	n/v	
[n]:	0.000000	11.92	0.000000	n/v	ml/g
Vp :	2.4166e1	11.92	2.5141e1	n/v	ml
Mp :	3.5493e4	11.92	2.1440e4	n/v	g/mol
FI :	7.2417e3	11.92	1.0091e0	n/v	ml*V
< 3340	0.00	11.92	0.00	n/v	
w% :	100.00	11.92	100.00	n/v	
> 166020	0.00	11.92	0.00	n/v	

Projekt :	C:\GPC-Daten\Installation.LDX		**Kostenstelle :**
Datum :	Montag 29.02.16 14:48:33		**Zeichen :**

Fig. S19 GPC chromatogram of PLA (sample Table 2, Entry 10).

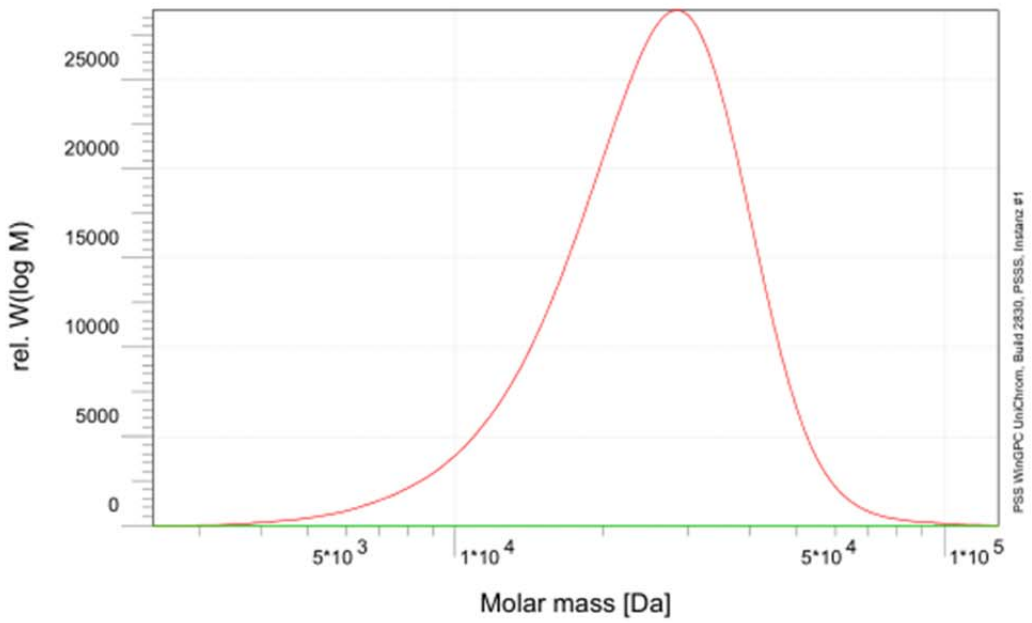

Probe :	Vial 1: WR/513/1 - 1		
Integration von :	Montag 18.05.15 09:45:40		21.712 ml
Integration bis :	Montag 18.05.15 09:53:15		29.484 ml
Kalibration :	thf20132406.CAL	**Eluent :**	THF
MHK - A (Kal.):	1.000E+0	**MHK - K (Kal.):**	0.000E+0 ml/g
Int.Stand.-K :	37.250 ml	**Int.Stand.-M :**	36.284 ml
Pumpe :	PSS SECcurity	**Flußrate :**	1.000 ml/min
Konzentration :	0.000 g/l	**Injektvolumen :**	20.000 ul
Säule 1 :	PSS SDV 5µm	**Temperatur :**	25.000 °C
Säule 2 :	PSS SDV 5µm	**Temperatur :**	25.000 °C
Säule 3 :	PSS SDV 5µm	**Temperatur :**	25.000 °C
Detektor 1 :	I1: RID 1, RI Signal	**Versatz :**	0.217 ml
Detektor 2 :	I1: VWD 1, Signal A	**Versatz :**	0.000 ml
Operateur :	mpaul	**Messintervall :**	1.000 sec

	I1: RID 1, RI Signal		**I1: VWD 1, Signal A**		
		Unsicherheit [%]		**Unsicherheit [%]**	
Mn :	2.1822e4	4.04	1.5553e4	n/v	g/mol
Mw :	2.7027e4	4.04	2.3501e4	n/v	g/mol
Mz :	3.2042e4	4.04	3.3252e4	n/v	g/mol
Mv :	2.7027e4	4.04	2.3501e4	n/v	g/mol
D :	1.2385e0	5.71	1.5110e0	n/v	
[n]:	0.000000	4.04	0.000000	n/v	ml/g
Vp :	2.4588e1	4.04	2.4743e1	n/v	ml
Mp :	2.8519e4	4.04	2.6332e4	n/v	g/mol
FI :	1.2958e4	4.04	6.003e-1	n/v	ml*V
< 2406	0.00	4.04	0.00	n/v	
w% :	100.00	4.04	100.00	n/v	
> 128884	0.00	4.04	0.00	n/v	

Projekt :	C:\GPC-Daten\Installation.LDX		**Kostenstelle :**
Datum :	Montag 29.02.16 14:46:38		**Zeichen :**

Fig. S20 GPC chromatogram of PCL (sample Table 2, Entry 17).

6. Redox Reactions

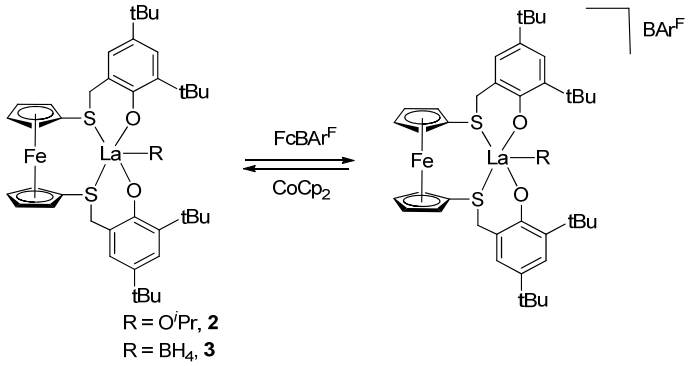

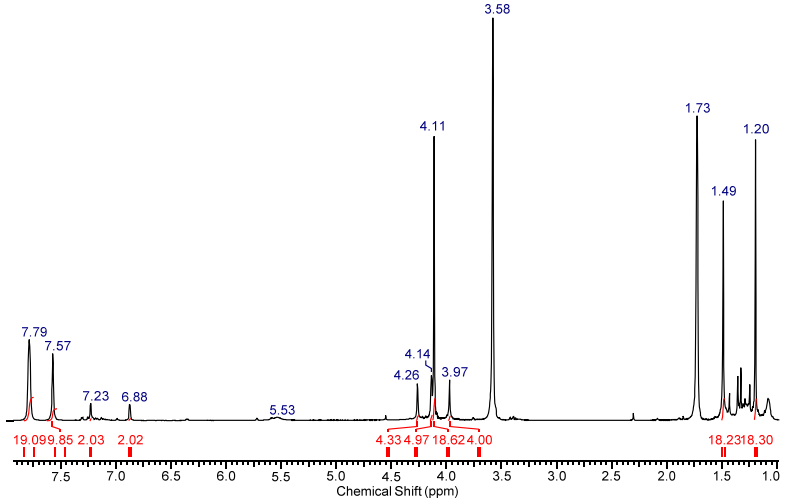

Fig. S21 ^{1}H NMR spectrum (THF-d_8, 400 MHz) of complex **2** after adding one equivalent of FcBAr^F.

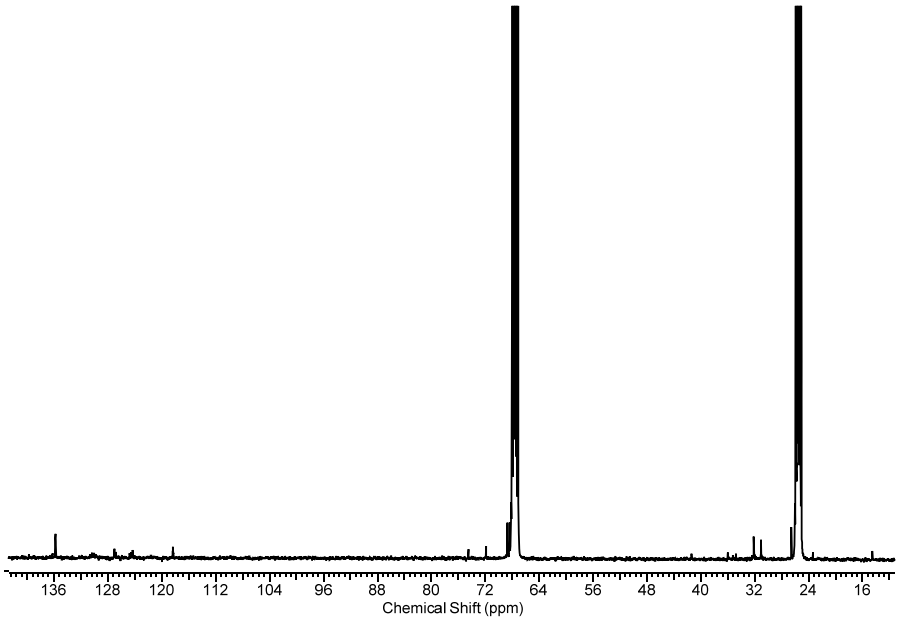

Fig S 22 ^{13}C {^{1}H} NMR spectrum (THF-d_8, 400 MHz) of complex **2** after adding one equivalent of FcBAr^F.

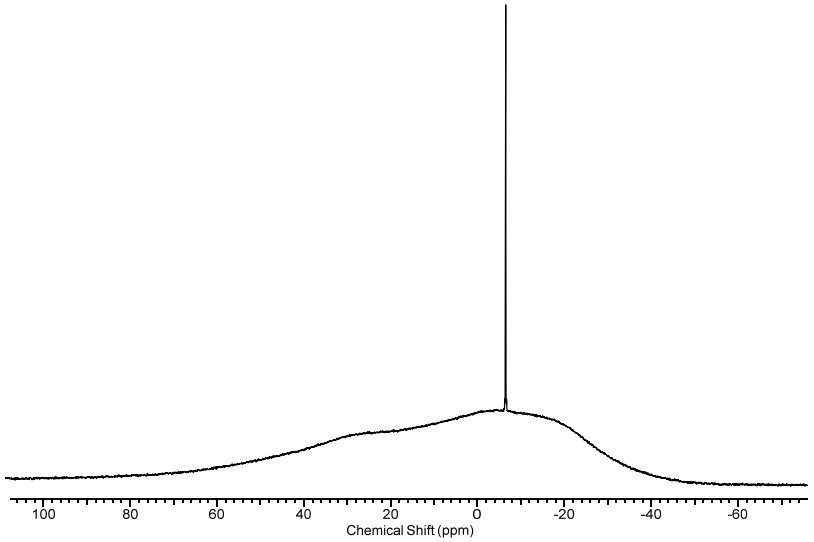

Fig. S23 ^{11}B {^{1}H} NMR spectrum (THF-d_8, 400 MHz) of complex **2** after adding one equivalent of FcBAr^{F}.

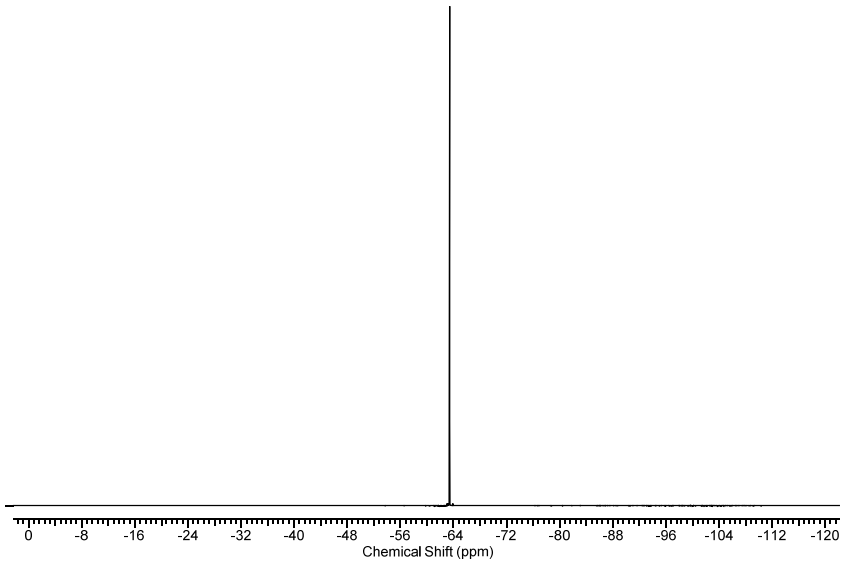

Fig. S24 ^{19}F {^{1}H} NMR spectrum (THF-d_8, 400 MHz) of complex **2** after adding one equivalent of FcBAr^{F}.

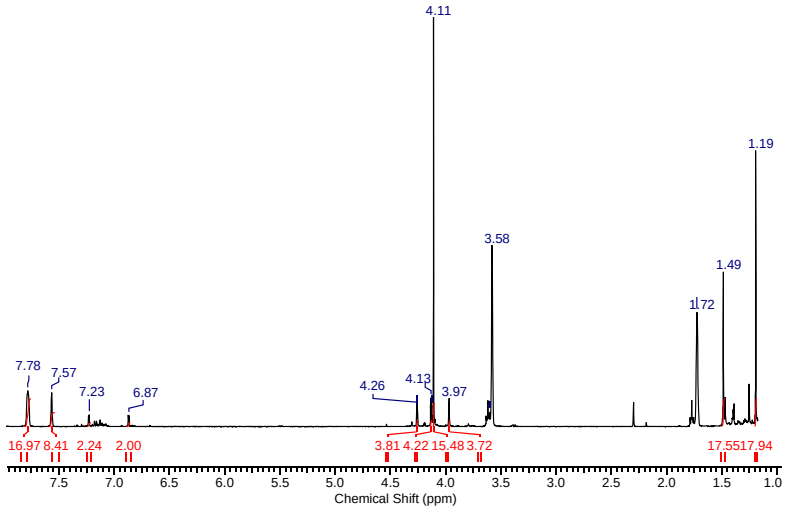

Fig. S25 ^{1}H NMR spectrum (THF-d_8, 400 MHz) of complex **3** after adding one equivalent of FcBAr^{F}.

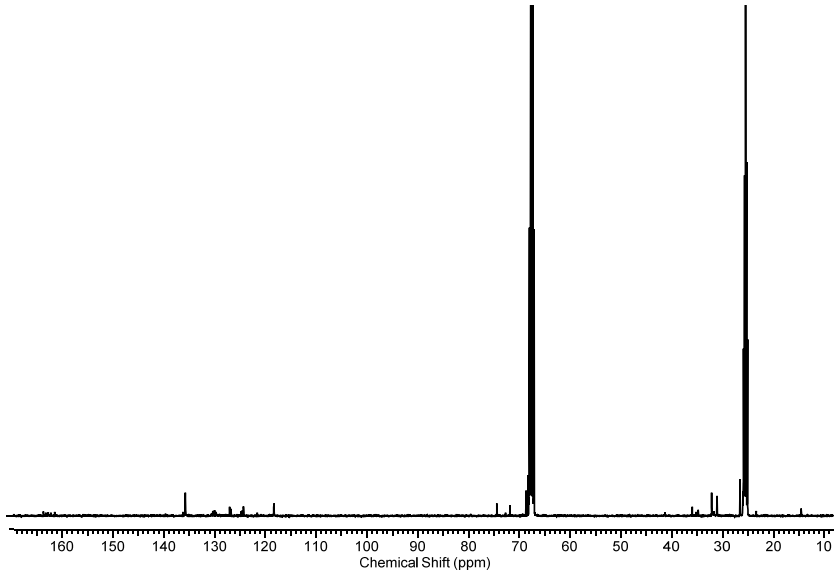

Fig. S26 ^{13}C {^{1}H} NMR spectrum (THF-d_8, 400 MHz) of complex **3** after adding one equivalent of $FcBAr^F$.

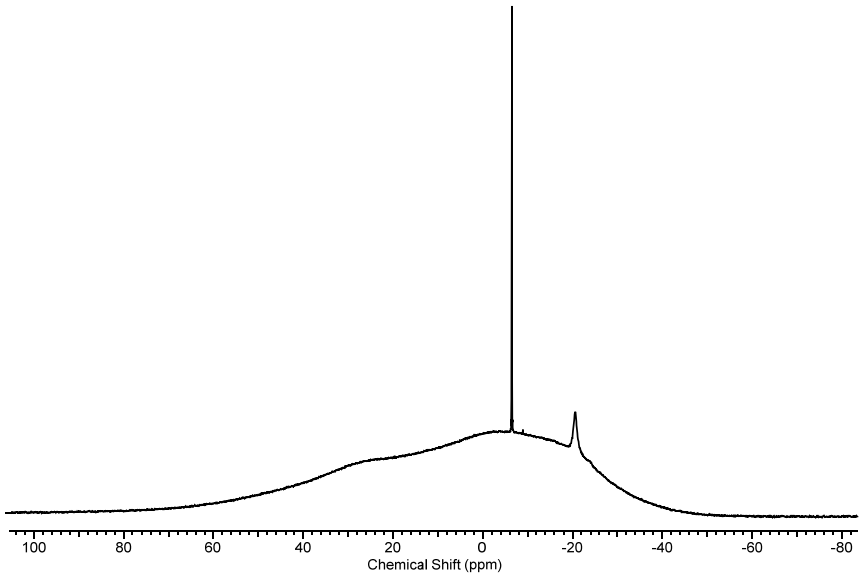

Fig. S27 ^{11}B {^{1}H} NMR spectrum (THF-d_8, 400 MHz) of complex **3** after adding one equivalent of $FcBAr^F$.

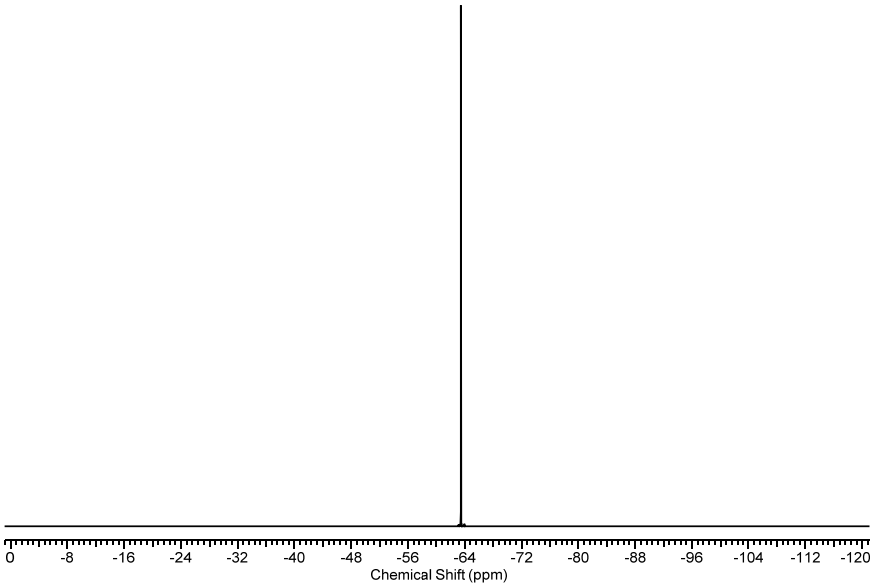

Fig. S28 ^{19}F $\{^{1}H\}$ NMR spectrum (THF-d_8, 400 MHz) of complex **3** after adding one equivalent of $FcBAr^{F}$.

7. Crystallography

X-ray diffraction data were collected on a Bruker CCD area-detector diffractometer with Mo Kα radiation (monolayer optics, λ = 0.71073 Å) using ω scans.[S1] The SMART program package was used for the data collection and unit cell determination; processing of the raw frame data was performed using SAINT; absorption corrections were applied with SADABS.[S2] The structures were solved by direct methods (SIR-92).[S3] All non-hydrogen atoms were refined anisotropically using all reflections with the program SHELXL-2013 as implemented in the program system WinGX.[S4] All hydrogen atoms were placed in calculated positions and treated as riding. The graphical representations were performed with the program DIAMOND.[S5]

Table S1 Crystallographic data and structure refinement details for complex **1**

	1 · C_6H_{14}
formula	$C_{46}H_{70}FeLaNO_2S_2Si_2 \cdot C_6H_{14}$
M_w	1070.26
cryst. system and space group	monoclinic, $P\,2_1/c$
a [Å]	10.0044(10)
b [Å]	29.326(3)
c [Å]	19.1690(19)
β [°]	92.678(2)
V [Å^3]	5617.8(10)
Z	4
d_{calcd} [g cm^{-3}]	1.265
radiation (λ [Å])	MoKα (0.71073)
$2\vartheta_{max}$ [°]	55.8
μ [mm^{-1}]	1.16
F [000]	2248
T_{min}, T_{max}	0.533, 0.746
reflns	67369 (R_{int} = 0.0899)
indep. reflns	12368
obs. reflns with $I > 2\sigma(I)$	9220
parameters refined	570
GOF	1.047
$R1$, w$R2$ for $I > 2\sigma(I)$	0.0423, 0.0905
$R1$, w$R2$ for all data	0.0697, 0.0957
Δe_{max}, Δe_{min} [e Å^{-3}]	0.952, - 0.654

8. Cyclic Voltammograms

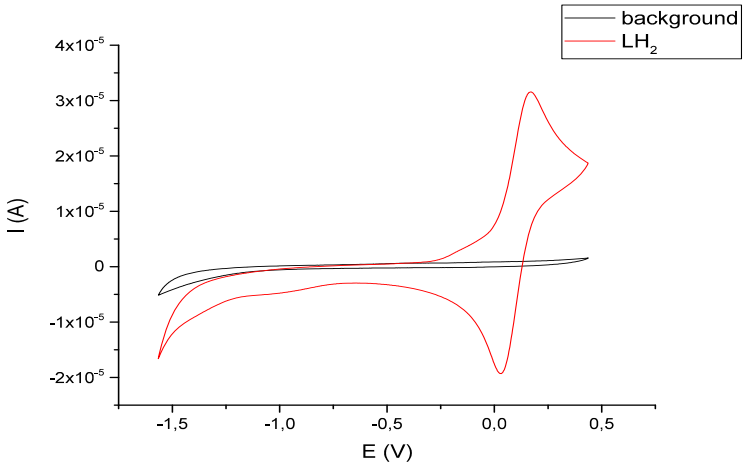

Fig S29a Cyclic voltammogram of LH_2, background (black), complex (red) vs ferrocene/ferrocenium (2.0 mmol/L in 1,2-difluorobenzene, 200 mV/s scan rate, 0.10 mol/L $[N^nBu_4][B(C_6F_5)_4]$).

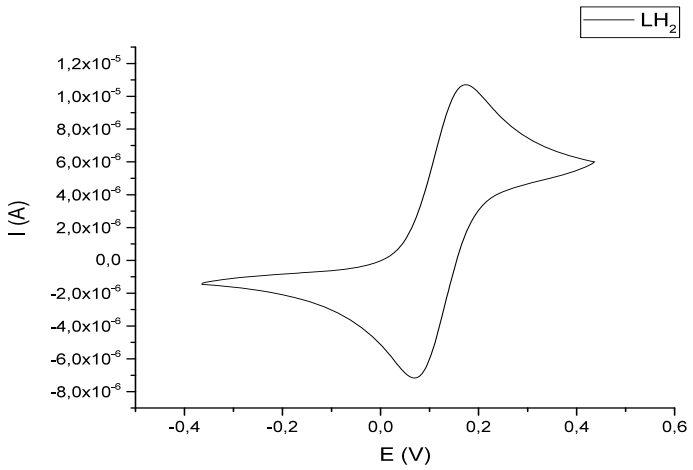

Fig S29b Cyclic voltammogram of LH_2 vs ferrocene/ferrocenium, $E_{1/2}$ = 0.11 V (2.0 mmol/L in 1,2-difluorobenzene, 20 mV/s scan rate, 0.10 mol/L $[N^nBu_4][B(C_6F_5)_4]$).

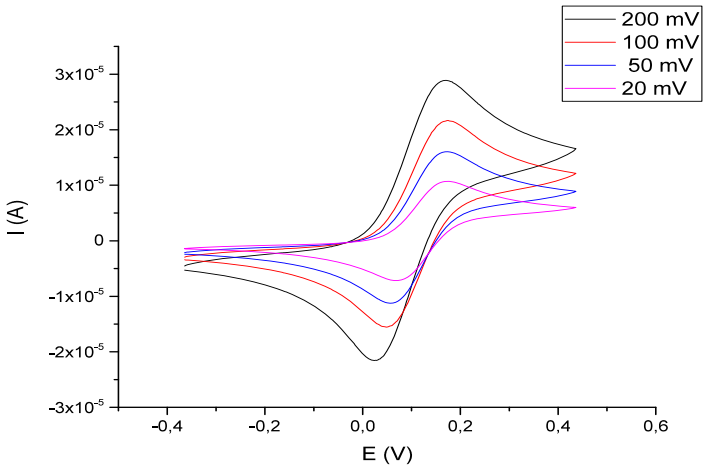

Fig S29c Cyclic voltammogram of LH_2 vs ferrocene/ferrocenium, 20 mV/s scan rate (purple), 50 mV/s scan rate (blue), 100 mV/s scan rate (red), 200 mV/s scan rate (black), $E_{1/2}$ = 0.11 V (2.0 mmol/L in 1,2-difluorobenzene, 0.10 mol/L $[N^nBu_4][B(C_6F_5)_4]$).

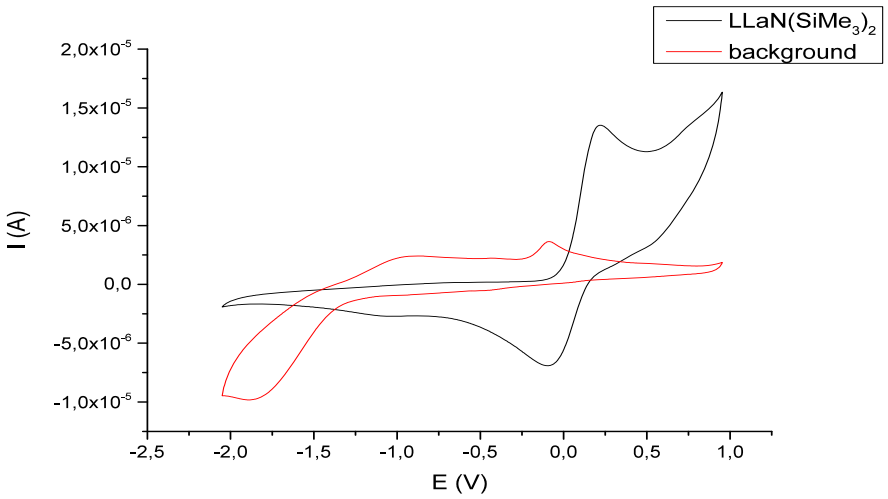

Fig. S30a Cyclic voltammogram of $LLaN(SiMe_3)_2$ (**1**), background (red), complex (black) vs ferrocene/ferrocenium (2.0 mmol/L in 1,2-difluorobenzene, 200 mV/s scan rate, 0.10 mol/L $[N^nBu_4][B(C_6F_5)_4]$).

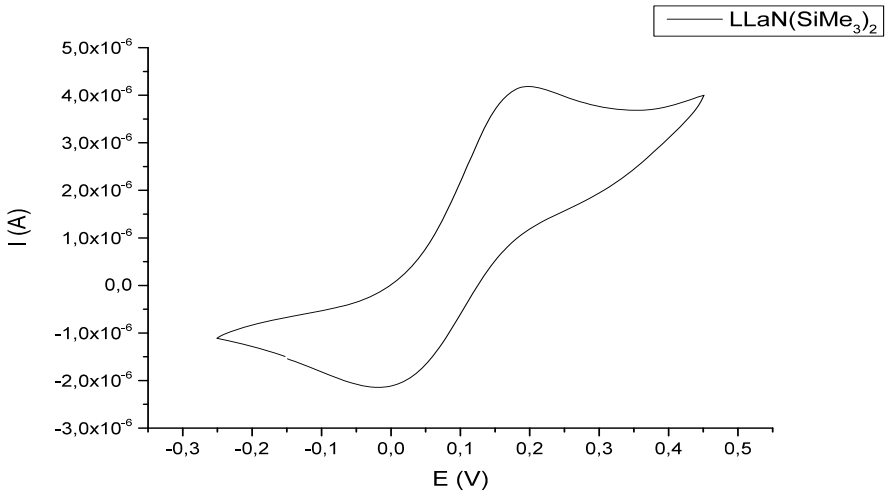

Fig. S30b Cyclic voltammogram of **1** vs ferrocene/ferrocenium, $E_{1/2}$ = 0.093 V (2.0 mmol/L in 1,2-difluorobenzene, 20 mV/s scan rate, 0.10 mol/L $[N^nBu_4][B(C_6F_5)_4]$).

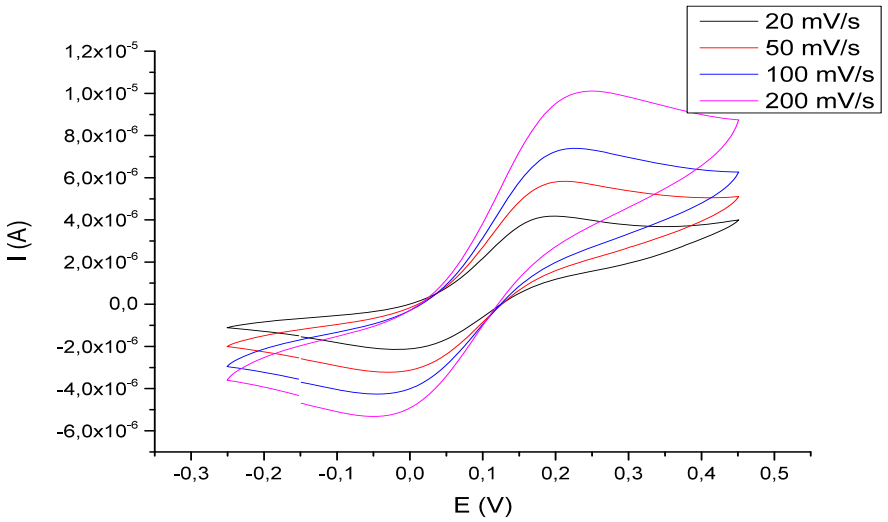

Fig. S30c Cyclic voltammogram of **1** vs ferrocene/ferrocenium, 20 mV/s scan rate (black), 50 mV/s scan rate (red), 100 mV/s scan rate (blue), 200 mV/s scan rate (purple), $E_{1/2}$ = 0.093 V (2.0 mmol/L in 1,2-difluorobenzene, 0.10 mol/L $[N^nBu_4][B(C_6F_5)_4]$).

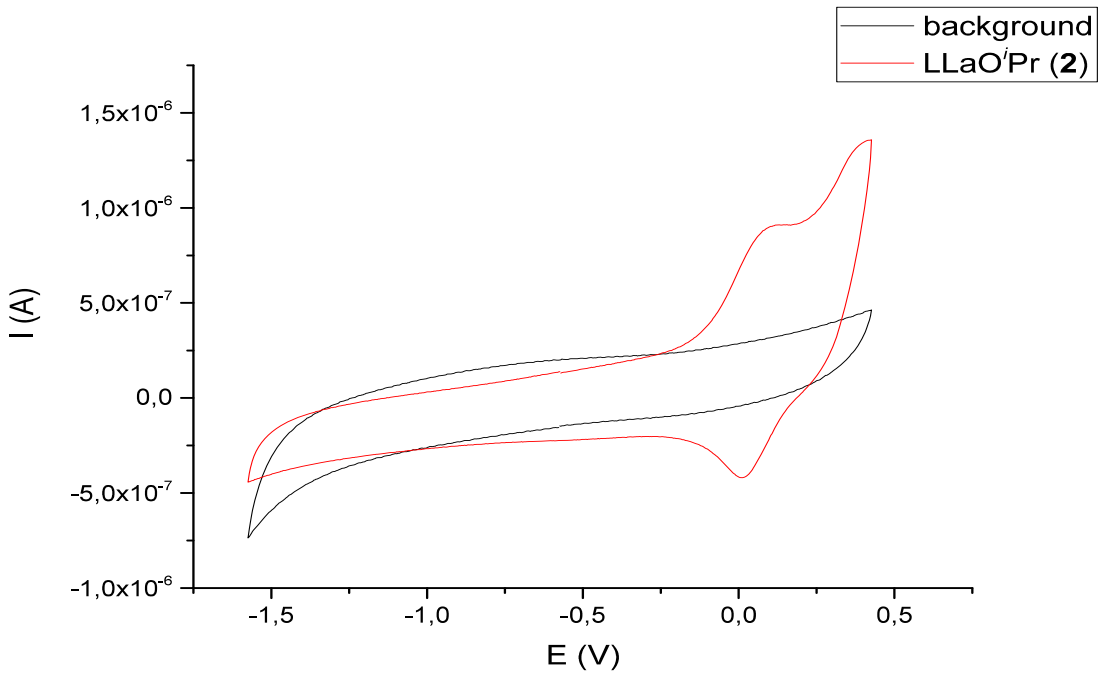

Fig. S31a Cyclic voltammogram of **2**, background (red), complex (black) vs ferrocene/ferrocenium (2.0 mmol/L in 1,2-difluorobenzene, 200 mV/s scan rate, 0.10 mol/L [N^{n}Bu$_4$][B(C$_6$F$_5$)$_4$).

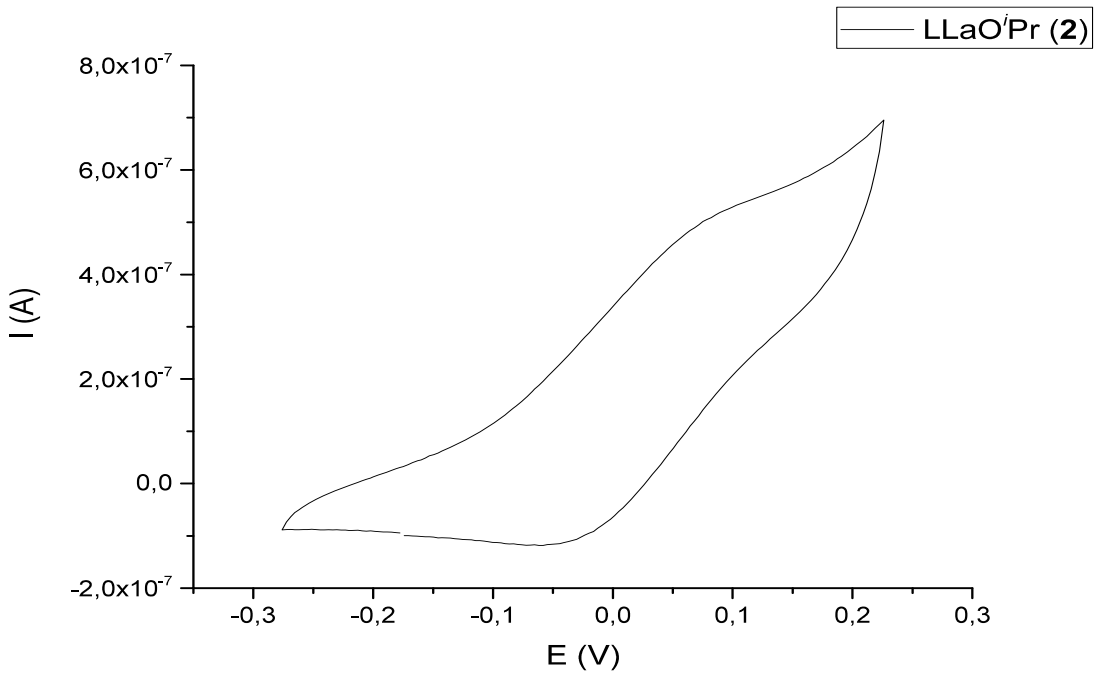

Fig. S31b Cyclic voltammogram of **2** vs ferrocene/ferrocenium, $E_{1/2}$ = 0.055 V (2.0 mmol/L in 1,2-difluorobenzene, 20 mV/s scan rate, 0.10 mol/L [N^{n}Bu$_4$][B(C$_6$F$_5$)$_4$]).

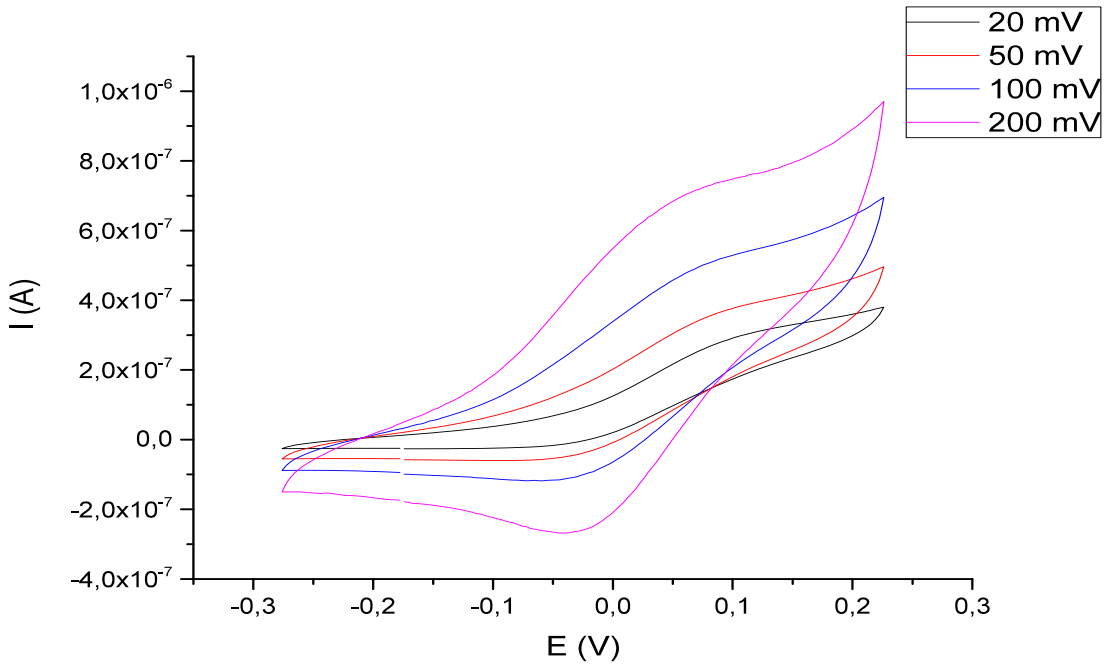

Fig. S31c Cyclic voltammogram of **2** vs ferrocene/ferrocenium, 20 mV/s scan rate (black), 50 mV/s scan rate (red), 100 mV/s scan rate (blue), 200 mV/s scan rate (purple), $E_{1/2}$ = 0.055 V (2.0 mmol/L in 1,2-difluorobenzene, 0.10 mol/L [N^nBu_4][$B(C_6F_5)_4$]).

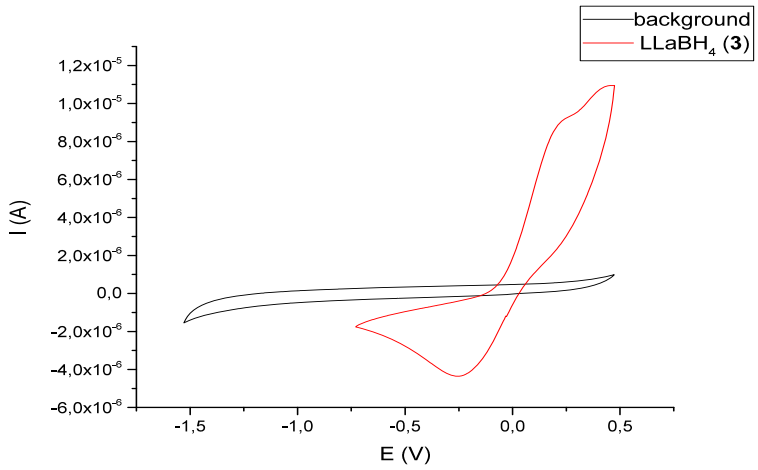

Fig. S32a Cyclic voltammogram of **3**, background (black), complex (red) vs ferrocene/ferrocenium (2.0 mmol/L in 1,2-difluorobenzene, 200 mV/s scan rate, 0.10 mol/L [N^nBu_4][$B(C_6F_5)_4$]).

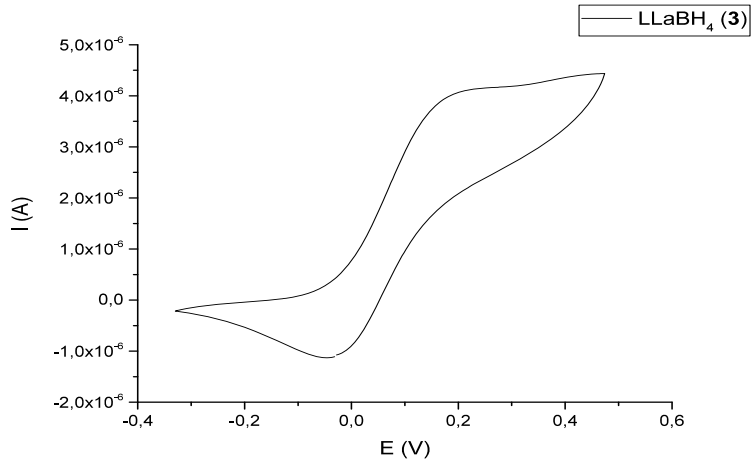

Fig. S32b Cyclic voltammogram of **3** vs ferrocene/ferrocenium, $E_{1/2}$ = 0.084 V (2.0 mmol/L in 1,2-difluorobenzene, 20 mV/s scan rate, 0.10 mol/L $[N^nBu_4][B(C_6F_5)_4]$).

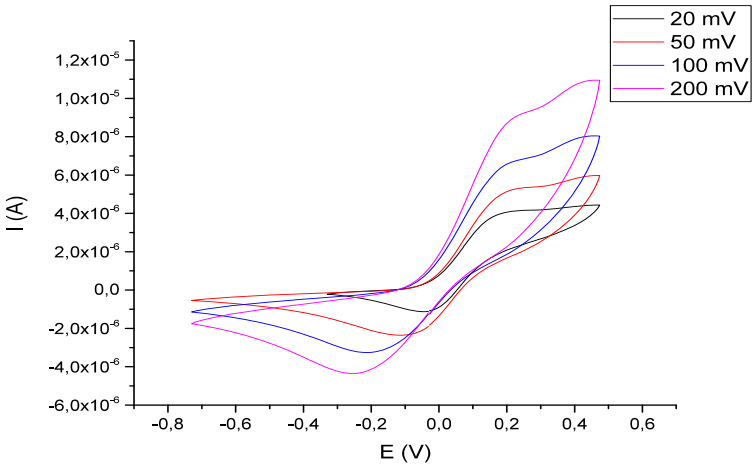

Fig. S32c Cyclic voltammogram of **3** vs ferrocene/ferrocenium, 20 mV/s scan rate (black), 50 mV/s scan rate (red), 100 mV/s scan rate (blue), 200 mV/s scan rate (purple), $E_{1/2}$ = 0.084 V (2.0 mmol/L in 1,2-difluorobenzene, 0.10 mol/L $[N^nBu_4][B(C_6F_5)_4]$).

9. References

S1. Bruker, SAINT-Plus, Bruker AXS Inc., Madison, Wisconsin, USA, 1999.

S2. Bruker, SADABS, Bruker AXS Inc., Madison, Wisconsin, USA, 2004.

S3. A. Altomare, G. Cascarano, C. Giacovazzo, A. Guagliardi, M. c. Burla, G. Polidori and M. Camalli, *J. Appl. Cryst.*, 1994, **27**, 435-436.

S4. (a) G. M. Sheldrick, *Acta. Cryst.*, 2008, **A64**, 112-122. (b) L. J. Farrugia, *J. Appl. Cryst.*, 1999, **32**, 837-838.

S5. K. Brandenburg, Diamond, Crystal Impact GbR, Bonn (Germany), 2004.